



RESEARCH LETTER

10.1029/2018GL080879

Soil Moisture Effects on Afternoon Precipitation Occurrence in Current Climate Models

Heewon Moon¹ , Benoit P. Guillod^{1,2} , Lukas Gudmundsson¹ , and Sonia I. Seneviratne¹ ¹Institute for Atmospheric and Climate Science, ETH Zurich, Zurich, Switzerland, ²Institute for Environmental Decisions, ETH Zurich, Zurich, Switzerland

Key Points:

- Climate models simulate strong positive spatial soil moisture-precipitation (SMP) feedback as opposed to observations
- Intermodel variability in temporal and heterogeneity characteristics of SMP feedback metrics is large
- SMP feedback biases in models might contribute to longer localized daily precipitation persistence than in observations

Supporting Information:

- Supporting Information S1

Correspondence to:

H. Moon,
heewon.moon@env.ethz.ch

Citation:

Moon, H., Guillod, B. P., Gudmundsson, L., & Seneviratne, S. I. (2019). Soil moisture effects on afternoon precipitation occurrence in current climate models. *Geophysical Research Letters*, 46, 1861–1869. <https://doi.org/10.1029/2018GL080879>

Received 15 OCT 2018

Accepted 20 JAN 2019

Accepted article online 28 JAN 2019

Published online 14 FEB 2019

Abstract Soil moisture-precipitation feedbacks in a large ensemble of global climate model simulations are evaluated. A set of three metrics are used to assess the sensitivity of afternoon rainfall occurrence to morning soil moisture in terms of their spatial, temporal, and heterogeneity characteristics. Positive (negative) spatial feedback indicates that the afternoon rainfall occurs more frequently over wetter (drier) land surface than its surroundings. Positive (negative) temporal feedback indicates preference over temporally wetter (drier) conditions, and positive (negative) heterogeneity feedback indicates preference over more spatially heterogeneous (homogeneous) soil moisture conditions. We confirm previous results highlighting a dominantly positive spatial feedback in the models as opposed to observations. On average, models tend to agree better with observations for temporal and heterogeneity feedback characteristics, although intermodel variability is largest for these metrics. The collective influence of the three feedbacks suggests that they may lead to more localized precipitation persistence in models than in observations.

Plain Language Summary Not only does rainfall influence soil moisture, but soil moisture can also actively influence rainfall. Current climate models do not represent such two-way relationships correctly, mainly due to uncertainty in the latter. Our understanding of models' weaknesses in simulating these processes is relatively low, and this is the focus of this study. Here we investigate how afternoon rainfall occurrence is affected by morning soil moisture conditions from three perspectives: relative soil moisture of the region where it rains compared to (1) surrounding regions (spatial feedback), (2) its long-term mean (temporal feedback), and (3) the spatial heterogeneity of soil moisture (heterogeneity feedback). In models, the afternoon rainfall preferably occurs over regions that are wetter than their surroundings, as opposed to observations. Models show better agreement with observations in the temporal and heterogeneity feedback, but large differences across the models remain. We suggest that the combined effect of these three relationships in models may contribute to their biases in the persistence of precipitation.

1. Introduction

Despite substantial research over the past few decades, soil moisture-precipitation (hereafter SMP) feedbacks remain among the most uncertain processes in the field of land-atmospheric interactions (Santanello et al., 2017; Seneviratne et al., 2010). Soil moisture influence on precipitation at seasonal to interannual scales has been investigated with the concept of moisture recycling (Dirmeyer et al., 2006; Eltahir & Bras, 1996; van der Ent et al., 2010), here referred to as direct SMP feedback. There has also been an increasing attention toward understanding indirect SMP feedback at subdaily to daily scales, which is also the focus of our study. Indirect SMP feedback can be narrowed down to the influence of soil moisture condition on boundary layer characteristics and convective initiation. Several studies have investigated such local effects of soil moisture using two main types of approaches. Some focused on the temporal effect of soil moisture on rainfall based on one-dimensional frameworks, which can yield both positive and negative effects (Alfieri et al., 2008; Duerinck et al., 2016; Findell & Eltahir, 2003; Gentine et al., 2013; Guillod et al., 2014). A positive temporal feedback appears when the increase of moisture is more critical for the cloud formation and precipitation, often under low stability in the free troposphere. A negative temporal feedback usually appears under a strong stability barrier at the top of planetary boundary layer, which requires larger sensible heat to allow sufficient turbulent mixing (Hohenegger et al., 2009). Another line of research considers spatial soil moisture gradients (C. M. Taylor & Lebel, 1998) whereby locally drier soils induce a mesoscale atmospheric

©2019. The Authors.

This is an open access article under the terms of the Creative Commons Attribution-NonCommercial-NoDerivs License, which permits use and distribution in any medium, provided the original work is properly cited, the use is non-commercial and no modifications or adaptations are made.

circulation such that increased convergence over the drier region, which leads to convection (C. M. Taylor et al., 2011). Conceptually, temporal and spatial feedbacks may interact: Rainfall may produce spatial heterogeneities in soil moisture that subsequently lead to further rainfall events over the drier regions, thereby increasing precipitation occurrence over a wider area (Guillod et al., 2015; H. Hsu et al., 2017).

C. M. Taylor, de Jeu, et al. (2012) have demonstrated that observations display a negative spatial SMP feedback, contrary to global climate models (GCMs), which display a positive feedback. This misrepresentation of SMP feedback in GCMs suggests issues in the dynamics of rainfall and soil moisture and could introduce systematic errors in the climate simulated by these models. Many studies have assessed the feedback in GCMs using different approaches, including modeling experiments. Koster et al. (2006) investigated the relative strength of the SMP feedback across GCMs in terms of precipitation variability explained by soil moisture and highlighted regions with stronger coupling such as the Sahel and central North America. Several regional studies analyzed the development of convective rainfall in model simulations with different soil moisture perturbations, in, for example, South Africa (Cook et al., 2006), the Indian and African monsoon region (Douville et al., 2001; Meehl, 1994), the Alpine region (Hohenegger et al., 2009), and the Sahel (C. M. Taylor et al., 2013). These studies commonly concluded that simulations with parameterized convection, as applied in most of the GCMs, are not able to simulate negative feedbacks. In addition, although the previous studies have proven the substantial contribution of parameterized convection to SMP feedback in models, the role of the land surface schemes should not be overlooked as surface variability induced from land surface processes is likely to influence the development of convection and thus the SMP feedback itself.

Previous studies mainly point to the spatial resolution of models and thereby parameterization of convection as the main issue that may prevent GCMs from correctly simulating SMP feedbacks. Nonetheless, there is a lack of understanding in how such feedbacks are represented in current GCMs, especially with respect to their spatial and temporal components. In this study, for the first time we evaluate both spatial and temporal SMP feedbacks in a large ensemble of fully coupled climate models using the diagnostics introduced by C. M. Taylor, de Jeu, et al. (2012) and Guillod et al. (2015). Section 2 describes the observational data and models used in the analysis. Section 3 describes the coupling diagnostics and their application to both observations and models. The analysis of SMP feedbacks in observations and models is presented in section 4.1. In section 4.2, the possible collective effects of spatial and temporal SMP feedbacks in observations and models are discussed. Conclusions are drawn in section 5.

2. Data

2.1. Observational Data

In this study, three precipitation data sets and four soil moisture data sets are used, which resulted in 12 combinations of observational estimates of the SMP feedback metrics. Using multiple observational data sets allows to consider observational uncertainty in identifying the SMP feedback (Ford et al., 2018; Guillod et al., 2015). All observational data are sets commonly available over the period 2002–2011 at $0.25^\circ \times 0.25^\circ$ resolutions.

2.1.1. Precipitation

We use three different 3-hourly precipitation data sets that are commonly based on multiple satellite measurements: version 1.0 of the CMORPH (Climate Prediction Center morphing method, Joyce et al., 2004) precipitation product, PERSIANN (Precipitation Estimation from Remotely Sensed Information using Artificial Neural Networks, K.-L. Hsu et al., 1997), and version 7 of TRMM3B42 (from the Tropical Rainfall Measuring Mission, hereafter referred as TRMM, Huffman et al., 2007). CMORPH precipitation is derived by propagating infrared data from geostationary satellites to precipitation estimates obtained from passive microwave sensor aboard polar-orbiting satellites, which complement each other with their different advantages on detection accuracy and spatiotemporal coverage. The PERSIANN algorithm also uses combined infrared and passive microwave information from multiple geostationary and low Earth orbit satellites with an artificial neural network model of which parameters are updated with ground-based data. TRMM precipitation is a combined precipitation estimates from multiple satellite systems, which is adjusted with rain gauge observations. We adjusted the 3-hourly precipitation data sets to local time based on longitude before the analysis.

2.1.2. Soil Moisture Data

We use Land Parameter Retrieval Model (Owe et al., 2008) version of AMSR-E (The Advanced Microwave Scanning Radiometer for Earth Observing System) soil moisture (hereafter referred to as AMSR), and three different soil moisture estimates from GLEAM (Global Land Evaporation Amsterdam Model, Miralles et al. (2011)), the latter resulting from the use of three precipitation data sets described in the former section as an input to GLEAM.

The Land Parameter Retrieval Model is mainly based on the relationship between polarization ratios, vegetation optical depth, and the soil dielectric constant and the derived surface soil moisture represents the uppermost 1–1.5 cm, as the AMSR-E detects microwave brightness temperatures at X (8–12 GHz) and C band (4–8 GHz). We use the AMSR estimated at 1:30 a.m. local time, which is the descending overpass time of AMSR-E. The soil moisture from GLEAM is derived as evaporative stress representing the whole root zone depth using remotely sensed radiation, precipitation, air temperature, soil moisture, vegetation optical depth, and snow water equivalent as input. The GLEAM data used in this study (see also Hsu et al., 1997, 2015) assimilate AMSR soil moisture available for 2002–2011 period and were driven by the three different precipitation data sets used in this study. Since a soil moisture estimate at a specific timing of day (9 a.m.) is required for calculating the SMP feedback metrics, the original GLEAM formulation that provides estimates of daily averages (0–24 UTC) was modified such that the input variables are aggregated at a local daily cycle, which starts and ends at 9 a.m. local time and the estimated soil moisture hence corresponds to instantaneous values at 9 a.m. Further details of this specific version of GLEAM can be found in Guillod et al. (2015).

2.2. CMIP5 Models

GCM output data from historical simulations, for the period 1976–2005, from the CMIP5 (K. E. Taylor, Stouffer, et al., 2012) ensemble have been used. A longer time period (compared to observations) was necessary to ensure that enough afternoon rainfall events are captured in models, as their spatial resolutions are much coarser (see also section 3). Hence, we assume that SMP feedback characteristics have remained constant over the considered time period (1976–2011). Models with 3-hourly precipitation and surface soil moisture output available at a spatial resolution finer than $2.5^\circ \times 2.5^\circ$ were chosen, leading to the nine GCMs listed in Table 1 together with a few relevant properties. A longitude-based time adjustment was also conducted to ensure that model outputs are arranged along local time. The surface soil moisture output of the models used in this study represents the uppermost 10 cm, except for CNRM-CM5 of which represents the top 1 cm.

3. Coupling Diagnostic

Diagnostics to assess SMP coupling are mainly adopted from C. M. Taylor, de Jeu, et al. (2012) and Guillod et al. (2015). A set of three metrics, which assess the sensitivity of afternoon rainfall occurrence to morning soil moisture spatially, temporally and in terms of heterogeneity, are calculated for each afternoon precipitation event. In this section, we first provide a description of the methodology as applied to the observational data, and we then describe the differences introduced for the analysis of models at the end of this section.

For each day, accumulated afternoon precipitation (12 p.m. to 12 a.m.) is analyzed. Locations of precipitation maxima (L_{\max} , more than 4 mm) are first identified. An event domain ($Levt$) is subsequently defined as 5×5 grid cells centered at the L_{\max} locations, and locations of minimum rainfall on that day within $Levt$ are called L_{\min} . Grid cells with highly varying topography, water bodies or morning (6 a.m. to 12 p.m.) accumulated precipitation larger than 1 mm were masked out. The three metrics are then identified based on these locations as follows: The spatial metric Y_s is defined as $S'_{L_{\max}} - S'_{L_{\min}}$, where S' is the morning (preevent) soil moisture anomaly obtained by subtracting the seasonal cycle. The subscript refers to the location where S' is taken. The seasonal cycle of soil moisture was calculated by applying 31-day moving average filter to a multiyear daily climatology. In the case of multiple L_{\min} s due to zero precipitation, $S'_{L_{\min}}$ was calculated as the average soil moisture anomaly at all corresponding grid cells. The temporal metric Y_t is defined as $S'_{L_{\max}}$. The heterogeneity metric Y_h is defined as standard deviation of the 25 values, S'_{Levt} . Only the convective seasons determined by latitude are considered for the analysis, which are May–September for the north of 23°N , November–March for the south of 23°S , and all months in the tropics.

In addition to event samples that are metrics calculated for each event at the respective locations, we define a control sample as the same metrics at the same locations but from nonevent days from the same month of all years.

Table 1
Model Features Related to Atmospheric and Land Surface Scheme

Model name (main reference)	Resolution (° in latitude × ° in longitude)	Atmospheric model	Convection scheme	Land surface model (subgrid variability, number of soil layers)
ACCESS1-0 (Dix et al., 2013)	1.2 × 1.9	Included (as in HadGEM2(r1.1))	Mass flux scheme (Gregory & Rowntree, 1990)	MOSES2 (tiled, 4)
ACCESS1-3 (Dix et al., 2013)	1.2 × 1.9	Similar to GA1.0	Mass flux scheme (Gregory & Rowntree, 1990)	CABLE (tiled, 6)
CNRM-CM5 (Volodre et al., 2013)	1.4 × 1.4	ARPEGE-climat	Mass flux scheme (Bougeault, 1985)	SURFEX (tiled, 14)
HadGEM-ES2 (Collins et al., 2011)	1.2 × 1.9	Included	Mass flux scheme (Gregory & Rowntree, 1990)	MOSES2 (tiled, 4)
INMCM4 (Volodin et al., 2010)	1.5 × 2.0	Included	Convective adjustment scheme (Betts & Miller, 1986)	included
IPSL-CM5A-MR (Hourdin et al., 2013)	1.3 × 2.5	LMDZ5	Mass flux scheme (Emanuel, 1991)	ORCHIDEE (mosaic, 2)
MIROC5 (Watanabe et al., 2010)	1.4 × 1.4	CCSR/NIES/FRCGC AGCM6	Entraining plume model (Chikira & Sugiyama, 2010)	MATSIRO (single vegetation type per grid box, 13)
MRI-CGCM3 (Yukimoto et al., 2011)	1.1 × 1.1	MRI-AGCM3.3	Mass flux scheme (Yoshimura et al., 2015)	HAL (mosaic, 14)
MRI-ESM1 (Yukimoto et al., 2011)	1.1 × 1.1	MRI-AGCM3.3	Mass flux scheme (Yoshimura et al., 2015)	HAL (mosaic, 14)

All events within 5° × 5° boxes are pooled together to assess the statistical strength of the mean metric value, which is determined by assessing whether the differences between the event and control samples are significantly larger (or smaller) than those generated by chance as follows: First, the climatology of the individual locations within the 5° boxes is removed by subtracting the long-term mean of the values within the control and the event samples (pooled together from both samples for each location). Second, the difference between the averages of the event sample and the corresponding control sample ($\delta(Y) = \text{mean}(Y_e) - \text{mean}(Y_c)$) is computed, and its strength is determined by the corresponding quantile of the distribution of the same difference in each of 1,000 random samples. These samples consist of n values (where n is the size of the event sample) randomly selected from all values of the event and control samples pooled together (as a substitute for the event sample) and the remaining values within this pool (as a substitute for the control sample). Statistical significance of a positive (negative) feedback is claimed if the strength of $\delta(Y)$ is greater (smaller) than 0.9 (0.1). 5° boxes with less than 25 event samples were masked out as they cannot provide robust results.

The models and observations differ in terms of their spatial resolution. In addition, climate models consistently have an early initiation of afternoon rainfall compared to observations (Dai, 2006). To account for these mismatches, we follow previous assessments (C. M. Taylor, de Jeu, et al., 2012) and process observed and modeled data differently; time steps were used with a 3-hr shift in models (9 a.m. to 9 p.m. for afternoon, 3 a.m. to 9 a.m. for morning precipitation, and 6 a.m. to 9 a.m. for morning soil moisture), and Lev consists of 3 × 3 grid cells around Lmax instead of 5 × 5.

As mentioned earlier, the comparatively coarse spatial resolution of climate models requires parameterization of convection and this might itself affect the SMP feedback. We note that in previous studies (C. M. Taylor, de Jeu, et al., 2012), the metrics chosen to assess the SMP feedback were additionally calculated at coarser resolutions from observations, which resulted in weaker but consistent sign of the metrics. We find similar results in the supporting information (Figure S1), suggesting that the spatial resolution of the data

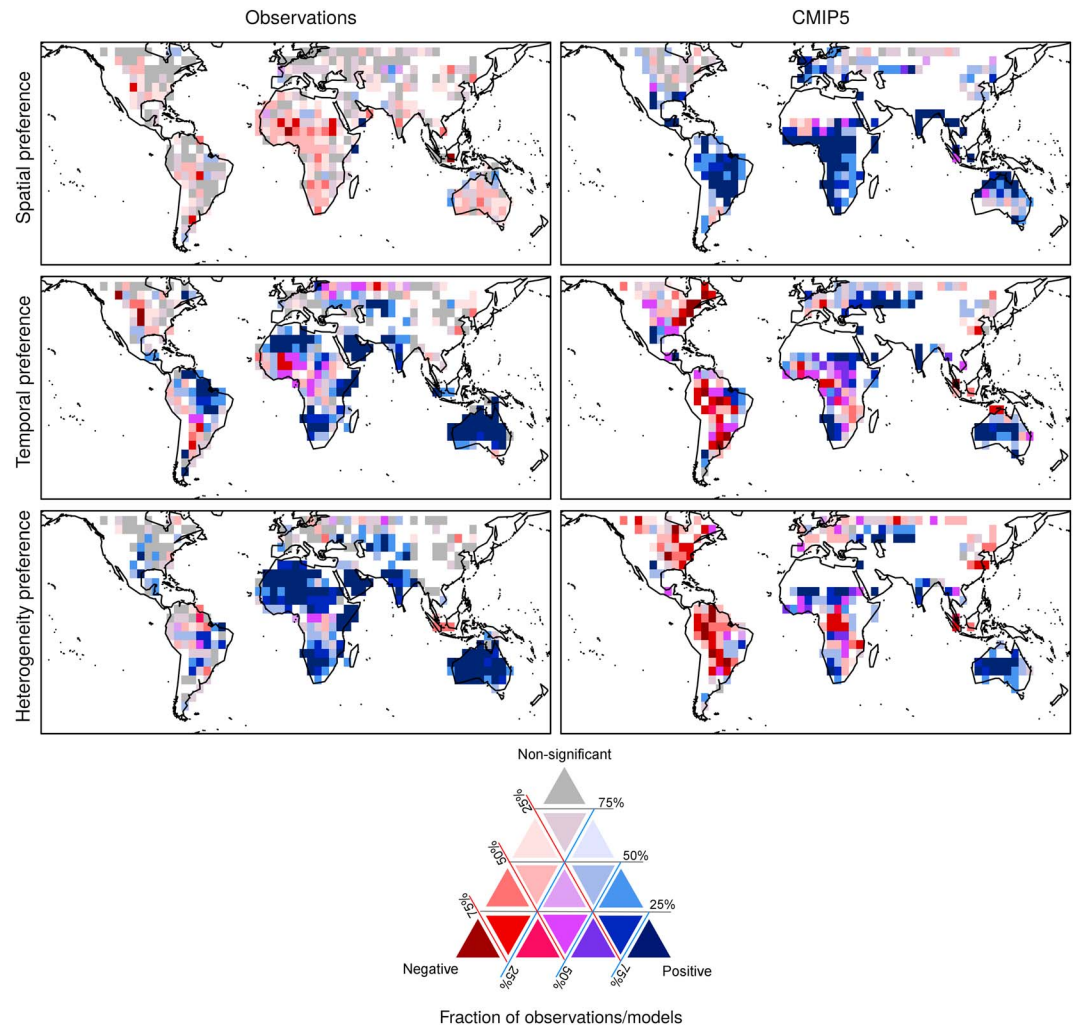


Figure 1. The three soil moisture-precipitation feedback metrics (from top to bottom: spatial, temporal, and heterogeneity metrics) in observations (left column) and CMIP5 models (right column). Colors are determined by the fraction of observation data set combinations or models in the following three categories: negative, nonsignificant, and positive with a 10% significance level. The 5° boxes with less than five valid observational or model soil moisture-precipitation feedback estimates were excluded.

on which the metrics are computed does not qualitatively affect the results. Nonetheless, the coarser spatial resolution of models compared to observations may cause the former to capture only the largest or most widespread events, while the observations capture many more smaller events. It should be noted that the metrics do not explicitly account for atmospheric preconditions (apart from the filter for morning rainfall, which ensures that rainfall was not already present in the morning), which might determine the preferred soil moisture condition or in some cases inhibit moist convection (Findell & Eltahir, 2003).

4. Results and Discussion

4.1. Average Statistics of Observations and Models

Figure 1 shows the fractions of observational estimates and models belonging to each of the categories of significantly positive (>0.9), significantly negative (<0.1) or nonsignificant feedbacks. Spatial SMP feedback (Y_s) in the models is dominantly positive as opposed to generally nonsignificant or negative Y_s in observations. The highest fraction of models simulating positive Y_s is found in South America, South Africa, and northern Australia. C. M. Taylor, de Jeu, et al. (2012) also found dominantly positive Y_s in model simulations of the Atmospheric Model Intercomparison Project that are forced with prescribed sea surface temperature. Some models still capture negative Y_s in the western part of Sahel, which appears as one of the regions with

the strongest negative Y_s in the observations. In North America and North Asia, most of the models simulate nonsignificant Y_s .

The temporal feedback (Y_t) in the models shows better agreement with observations than the other two feedback metrics. Positive Y_t in Australia, South Africa, North Asia, and India and negative Y_t in western South America and western Sahel are reasonably well captured by the models. Yet in North America the models show very different behavior compared to observations, with strong negative Y_t in the eastern part. Larger variability across the models is found in central North America, western and southern parts of Brazil, and central Africa (indicated by light purple). Note also that large-scale factors such as the North Atlantic Oscillation, El Niño/Southern Oscillation, or sea surface temperature variability could substantially affect precipitation persistence, which in turn may lead to a spurious correlation between soil moisture and subsequent precipitation (Guilod et al., 2014; Salvucci et al., 2002). For instance, precipitation persistence at the time scale of the order of weeks induced by oceanic or atmospheric processes could lead to a positive temporal metric even in the absence of SMP feedback mechanism (Orlowsky & Seneviratne, 2010; Tuttle & Salvucci, 2017). Although we cannot exclude such artifacts, the temporal feedback metric allows for a comparison between observations and models while providing an indication on the temporal feedback (Guilod et al., 2015). We note that the temporal metric also exhibits a negative sign in some regions, for example, parts of the Sahel and Southern Great Plains, indicating that the metric does not systematically identify positive coupling mechanisms.

While the heterogeneity feedback (Y_h) is dominantly positive or nonsignificant in observations, around 50% of the models capture positive Y_h correctly but show negative Y_h in most of the regions where observations indicate nonsignificant Y_h . In observations, Y_t and Y_h generally have a positive sign, if statistically significant. In the models, similarity between Y_t and Y_h is much stronger than in observations.

The feedback metrics for individual observations and models are shown in Figures S2 and S3 (supporting information), respectively. Interproduct variability is relatively large, and clusters of model families can be identified (see also Text S1). In addition, we note that observations and models also show substantially different spatial coverage of the feedback metrics, reflecting that a lower number of events are detected in several models (Figure S3, supporting information), since the same threshold for the minimum number of events is applied for both models and observation to ensure the statistical significance of estimated SMP feedback metrics. These differences in the number of analyzed precipitation events can be due to differences in spatial resolution (leading to more events in observations compared to models) and in the length of the time series (more events in models). In addition, a part of the difference may be due to the known drizzle issue, that is, an overestimated frequency of light intensity precipitation, in GCMs (Dai, 2006; Rosa & Collins, 2013). Hence, masking out the days with morning precipitation could be more critical for SMP diagnostics in the models.

4.2. Combined Effects of SMP Feedbacks

Figure 2 shows the fraction of land areas that feature combinations of the spatial and temporal SMP feedback metrics (top row) and heterogeneity feedback metric (bottom row) in observations and models. Results of the same analysis using different significant levels are presented in the supporting information (Figures S4 and S5). Only $5^\circ \times 5^\circ$ boxes of which more than a third are land areas were classified as land are considered, and the ratio of land area is calculated with area-weighted composition. Analyzing Y_s and Y_t in a combined way allows for a more comprehensive comparison of the pre-rainfall morning soil moisture conditions between observations and models. Additionally, with the consideration of Y_h , we discuss possible mechanisms behind the commonly found combinations of SMP feedback metrics in both observations and models and how they potentially contribute to the spatial and temporal structure of precipitation persistence.

The combination of negative (hereafter, N) Y_s and positive (hereafter, P) Y_t occurs predominantly in the observations. While each observational estimate shows a similar fraction of land area, the regions where the combination appears vary across different observational data sets (Figure S2, supporting information). An important implication of this combination (N Y_s -P Y_t) is that the majority of the afternoon rainfall events occur when the whole event domain is anomalously wet, since the location of maximum afternoon precipitation occurs over a grid cell with positive soil moisture anomaly in the morning (P Y_t), while the surrounding grid cells have even higher soil moisture anomaly (N Y_s). Therefore, the dominant positive heterogeneity metric across all observed estimations (Figure 2, lower left) indicates high heterogeneity among positive soil moisture anomalies, which should be distinguished from high heterogeneity due to mixture of dry and wet

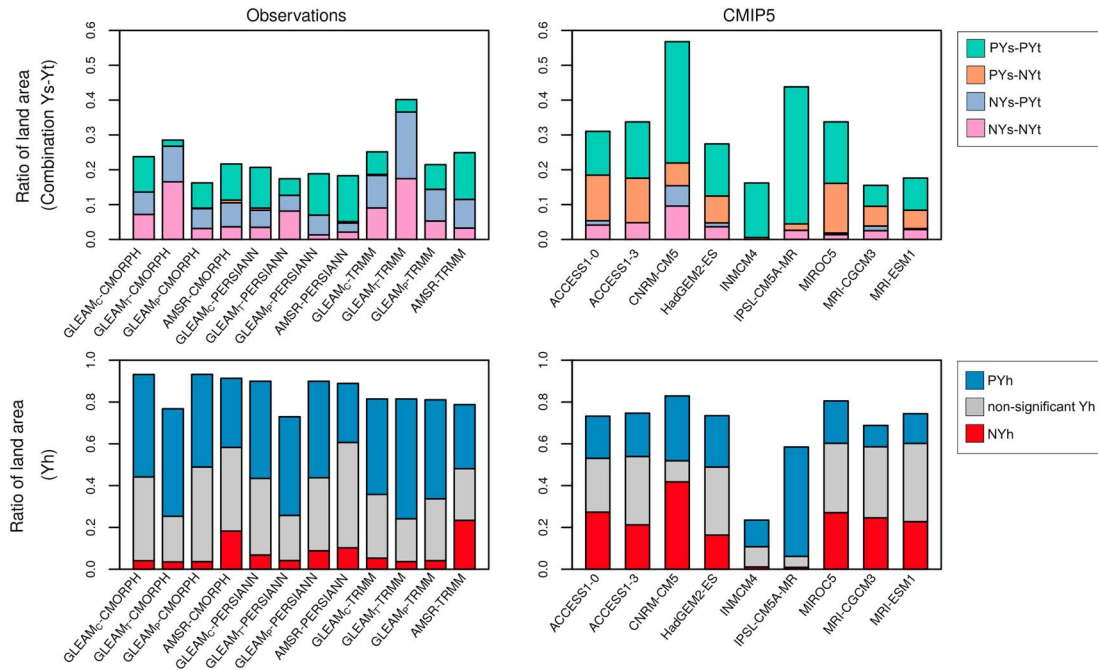


Figure 2. Fractions of land area with different combinations of the spatial and temporal soil moisture-precipitation feedback metrics (top row) and the heterogeneity feedback metric (bottom row) in observations and models. Ys, Yt, and Yh indicate spatial, temporal, and heterogeneity metric, respectively. P stands for positive sign of the feedback metrics and N for negative. Subscripts in GLEAM_c, GLEAM_t, and GLEAM_p indicate the precipitation data set used to derive each of the soil moisture estimates.

soil moisture anomalies. The other dominant combination in observations is NYs-NYt. This combination still reflects significantly more frequent afternoon rainfall occurrence over regions drier than their surroundings but also less precipitation persistence due to NYt. In addition, this combination does not reveal the large-scale soil moisture condition in the entire event domain, unlike the former, and thus, there is larger uncertainty in how the positive Yh is driven. It should be noted that in Figure 2, the combination of positive spatial and positive temporal metrics (PYs-PYt) also seems to appear relatively often. However, looking at the maps of the metrics (Figure S2) reveals that this cooccurrence in fact stems from various, randomly distributed grid cells and does not cluster into consistent regions. Therefore, this signal appears not robust and should be interpreted with caution.

In models, the combination of positive Ys and Yt (PYs-PYt) appears as the most common and is, unlike in observations, also confirmed by the maps in Figure S3. This combination indicates localized (grid scale) dry or wet persistence as it means that afternoon rainfall occurs more frequently over the temporally and spatially wetter regions. This is opposed to the observational estimates. PYs-NYt is the second most common combination in the models. PYs-NYt indicates that afternoon rainfall is more likely under dry soil condition and occurs over wetter regions in a given area. Thus, under this combination of feedbacks increase in precipitation likelihood might be only possible when there are sufficient drying down periods between the precipitation events, indicating a system with low precipitation persistence or high evaporative demands. The fraction of areas with different signs of Yh varies substantially across different models, but for each given model, the fractions of NYh and PYh are comparable. CNRM-CM5 appears as the only model where fraction of land areas with negative Ys and significant Yt is larger than 10%. IPSL-CM5A-MR simulates dominantly positive signals in all three metrics.

5. Conclusions

We evaluated spatial and temporal SMP feedbacks in nine GCMs stemming from the CMIP5 archive using three different metrics (Ys, Yt, and Yh), which quantify sensitivity of afternoon rainfall occurrence to morning soil moisture conditions compared to 12 observational estimates over the period of 1976–2011. We found dominantly positive spatial feedback metric (Ys) in all coupled climate models, contrasting to observations and consistent with the results of C. M. Taylor, de Jeu, et al. (2012), which were based on Atmospheric Model

Intercomparison Project-type simulations. The temporal feedback metric (Y_t) in the models shows better agreement with observations, but with a larger intermodel spread. When interpreting Y_t , one should keep in mind that the sign of the feedback metric might be partially caused by atmospheric persistence, which may induce spurious positive relationship between soil moisture and precipitation. The heterogeneity feedback metric (Y_h) and Y_t have similar spatial patterns in models, unlike in observations where Y_h is dominantly positive. The combinations of spatial and temporal SMP feedbacks in models, mainly PYS-PY $_t$ and PYS-NY $_t$, indicate that they might introduce more localized and stronger wet or dry persistence than the observations, where generally negative Y_s is combined with positive Y_h . The SMP feedback is an emergent property of climate models which is not parameterized and certainly influences simulated climate or weather phenomena. In particular, it reveals the spatiotemporal structure of precipitation persistence that could be favored in a given climate model. Thus, the results in this study may help to understand how land-climate interaction in climate models contributes to errors in precipitation variability at different temporal scales that were identified in previous investigations (Langford et al., 2014; Moon et al., 2018), of which substantial parts are not explained by contributions from large-scale variability.

Acknowledgments

We would like to thank the two anonymous reviewers for constructive comments. We acknowledge the World Climate Research Programme's Working Group on Coupled Modelling, which is responsible for CMIP, and we thank the climate modeling groups for producing and making available their model output which are available at <https://esgf-node.llnl.gov/search/cmip5/>. For CMIP the U.S. Department of Energy's Program for Climate Model Diagnosis and Intercomparison provides coordinating support and led development of software infrastructure in partnership with the Global Organization for Earth System Science Portals. We thank Urs Beyerle for the retrieval and preparation of CMIP5 model data. We also acknowledge the providers of observation data of the following products: CMORPH (ftp://ftp.cpc.ncep.noaa.gov/precip/global_CMORPH/3-hourly_025deg), GLEAM (<https://www.gleam.eu/>), AMSR-E (<https://www.geo.vu.nl/jeur/lprm/>). We also thank Robert M. Parinussa for providing the daily AMSR-E data from LPRM in local time and Diego Miralles for the derivation of before-noon evaporative stress estimates for Guillod et al. (2015) that are also used here. This study was supported by the European Research Council (ERC) "DROUGHT-HEAT" project funded through the European Community's Seventh Framework Programme (grant agreement FP7-IDEAS-ERC-617518).

References

Alfieri, L., Claps, P., D'Odorico, P., Laio, F., & Over, T. M. (2008). An analysis of the soil moisture feedback on convective and stratiform precipitation. *Journal of Hydrometeorology*, 9(2), 280–291. <https://doi.org/10.1175/2007JHM863.1>

Chikira, M. (2010). A cumulus parameterization with state-dependent entrainment rate. Part II: Impact on climatology in a general circulation model. *Journal of the Atmospheric Sciences*, 67(7), 2194–2211. <https://doi.org/10.1175/2010JAS3317.1>

Collins, W. J., Bellouin, N., Doutriaux-Boucher, M., Gedney, N., Halloran, P., Hinton, T., et al. (2011). Development and evaluation of an Earth-System model—HadGEM2. *Geosci. Model Dev.*, 4(4), 1051–1075. <https://doi.org/10.5194/gmd-4-1051-2011>

Cook, B. I., Bonan, G. B., & Levis, S. (2006). Soil moisture feedbacks to precipitation in southern Africa. *Journal of Climate*, 19(17), 4198–4206. <https://doi.org/10.1175/JCLI3856.1>

Dai, A. (2006). Precipitation characteristics in eighteen coupled climate models. *Journal of Climate*, 19(18), 4605–4630.

Dirmeyer, P. A., Koster, R. D., & Guo, Z. (2006). Do global models properly represent the feedback between land and atmosphere? *J. Hydrometeorol.*, 7(6), 1177–1198. <https://doi.org/10.1175/JHM532.1>

Dix, M., Vohralik, P., Bi, D., Rashid, H., Marsland, S., O'Farrell, S., et al. (2013). The ACCESS coupled model: Documentation of core CMIP5 simulations and initial results. *Australian Meteorological and Oceanographic Journal*, 63(1), 83–99. <https://doi.org/10.22499/2.6301.006>

Douville, H., Chauvin, F., & Broqua, H. (2001). Influence of soil moisture on the Asian and African monsoons. Part I: Mean monsoon and daily precipitation. *J. Climate*, 14(11), 2381–2403. [https://doi.org/10.1175/1520-0442\(2001\)014<2381:IOSMOT>2.0.CO;2](https://doi.org/10.1175/1520-0442(2001)014<2381:IOSMOT>2.0.CO;2)

Duerinck, H. M., van der Ent, R. J., van de Giesen, N. C., Schoups, G., Babovic, V., & Yeh, P. J.-F. (2016). Observed soil moisture-precipitation feedback in Illinois: A systematic analysis over different scales. *Journal of Hydrometeorology*, 17(6), 1645–1660.

Eltahir, E. A. B., & Bras, R. L. (1996). Precipitation recycling. *Reviews of Geophysics*, 34(3), 367–378. <https://doi.org/10.1029/96RG01927>

Emanuel, K. A. (1991). A scheme for representing cumulus convection in large-scale models. *Journal of the Atmospheric Sciences*, 48(21), 2313–2329. [https://doi.org/10.1175/1520-0469\(1991\)048<2313:ASFRCC>2.0.CO;2](https://doi.org/10.1175/1520-0469(1991)048<2313:ASFRCC>2.0.CO;2)

Findell, K. L., & Eltahir, E. A. B. (2003). Atmospheric controls on soil moisture-boundary layer interactions. Part I: Framework development. *J. Hydrometeorol.*, 4(3), 552–569. [https://doi.org/10.1175/1525-7541\(2003\)004<0552:ACOSML>2.0.CO;2](https://doi.org/10.1175/1525-7541(2003)004<0552:ACOSML>2.0.CO;2)

Ford, T. W., Quiring, S. M., Thakur, B., Jogineedi, R., Houston, A., Yuan, S., et al. (2018). Evaluating soil moisture-precipitation interactions using remote sensing: A sensitivity analysis. *Journal of Hydrometeorology*, 19(8), 1237–1253. <https://doi.org/10.1175/JHM-D-17-0243.1>

Gentile, P., Holtslag, A. A. M., D'Andrea, F., & Ek, M. (2013). Surface and atmospheric controls on the onset of moist convection over land. *J. Hydrometeorol.*, 14(5), 1443–1462. <https://doi.org/10.1175/JHM-D-12-0137.1>

Guillod, B. P., Orlovsky, B., Miralles, D., Teuling, A. J., Blanken, P. D., Buchmann, N., et al. (2014). Land-surface controls on afternoon precipitation diagnosed from observational data: Uncertainties and confounding factors. *Atmospheric Chemistry and Physics*, 14(16), 8343–8367. <https://doi.org/10.5194/acp-14-8343-2014>

Guillod, B. P., Orlovsky, B., Miralles, D. G., Teuling, A. J., & Seneviratne, S. I. (2015). Reconciling spatial and temporal soil moisture effects on afternoon rainfall. *Nature Communications*, 6, 6443. <https://doi.org/10.1038/ncomms7443>

Hohenegger, C., Brockhaus, B., Bretherton, C. S., & Schär, C. (2009). The soil moisture-precipitation feedback in simulations with explicit and parameterized convection. *Journal of Climate*, 22(19), 5003–5020. <https://doi.org/10.1175/2009JCLI2604.1>

Hourdin, F., Foujols, M.-A., Codron, F., Guemas, V., Dufresne, J.-L., Bony, S., et al. (2013). Impact of the LMDZ atmospheric grid configuration on the climate and sensitivity of the IPSL-CM5a coupled model. *Climate Dynamics*, 40(9–10), 2167–2192. <https://doi.org/10.1007/s00382-012-1411-3>

Hsu, K.-L., Gao, X., Sorooshian, S., & Gupta, H. V. (1997). Precipitation estimation from remotely sensed information using artificial neural networks. *J. Appl. Meteorol.*, 36(9), 1176–1190. [https://doi.org/10.1175/1520-0450\(1997\)036<1176:PEFRSI>2.0.CO;2](https://doi.org/10.1175/1520-0450(1997)036<1176:PEFRSI>2.0.CO;2)

Hsu, H., Lo, M.-H., Guillod, B. P., Miralles, D. G., & Kumar, S. (2017). Relation between precipitation location and antecedent/subsequent soil moisture spatial patterns: Precipitation-soil moisture coupling. *Journal of Geophysical Research: Atmospheres*, 122, 6319–6328. <https://doi.org/10.1002/2016JD026042>

Huffman, G. J., Bolvin, D. T., Nelkin, E. J., Wolff, D. B., Adler, R. F., Gu, G., et al. (2007). The TRMM Multisatellite Precipitation Analysis (TMPA): Quasi-global, multiyear, combined-sensor precipitation estimates at fine scales. *J. Hydrometeorol.*, 8(1), 38–55. <https://doi.org/10.1175/JHM560.1>

Joyce, R. J., Janowiak, J. E., Arkin, P. A., & Xie, P. (2004). CMORPH: A method that produces global precipitation estimates from passive microwave and infrared data at high spatial and temporal resolution. *J. Hydrometeorol.*, 5(3), 487–503. [https://doi.org/10.1175/1525-7541\(2004\)005<0487:CAMTPG>2.0.CO;2](https://doi.org/10.1175/1525-7541(2004)005<0487:CAMTPG>2.0.CO;2)

Koster, R. D., Sud, Y. C., Guo, Z., Dirmeyer, P. A., Bonan, G., Oleson, K. W., et al. (2006). GLACE: The global land-atmosphere coupling experiment. Part I: Overview. *J. Hydrometeorol.*, 7(4), 590–610. <https://doi.org/10.1175/JHM510.1>

- Langford, S., Stevenson, S., & Noone, D. (2014). Analysis of low-frequency precipitation variability in CMIP5 historical simulations for southwestern North America. *Journal of Climate*, 27(7), 2735–2756. <https://doi.org/10.1175/JCLI-D-13-00317.1>
- Meehl, G. A. (1994). Influence of the land surface in the Asian summer monsoon: External conditions versus internal feedbacks. *J. Climate*, 7(7), 1033–1049. [https://doi.org/10.1175/1520-0442\(1994\)007<1033:IOTLSI>2.0.CO;2](https://doi.org/10.1175/1520-0442(1994)007<1033:IOTLSI>2.0.CO;2)
- Miralles, D. G., Holmes, T. R. H., De Jeu, R. A. M., Gash, J. H., Meesters, A. G. C. A., & Dolman, A. J. (2011). Global land-surface evaporation estimated from satellite-based observations. *Hydrology and Earth System Sciences*, 15(2), 453–469. <https://doi.org/10.5194/hess-15-453-2011>
- Moon, H., Gudmundsson, L., & Seneviratne, S. I. (2018). Drought persistence errors in global climate models. *Journal of Geophysical Research: Atmospheres*, 123, 3483–3496. <https://doi.org/10.1002/2017JD027577>
- Orlowsky, B., & Seneviratne, S. I. (2010). Statistical analyses of land-atmosphere feedbacks and their possible pitfalls. *Journal of Climate*, 23, 3918–3932. <https://doi.org/10.1175/2010JCLI3366.1>
- Owe, M., Jeu, R. d., & Holmes, T. (2008). Multisensor historical climatology of satellite-derived global land surface moisture. *Journal of Geophysical Research*, 113, F01002. <https://doi.org/10.1029/2007JF000769>
- Rosa, D., & Collins, W. D. (2013). A case study of subdaily simulated and observed continental convective precipitation: CMIP5 and multiscale global climate models comparison. *Geophysical Research Letters*, 40, 5999–6003. <https://doi.org/10.1002/2013GL057987>
- Salvucci, G. D., Saleem, J. A., & Kaufmann, R. (2002). Investigating soil moisture feedbacks on precipitation with tests of Granger causality. *Adv. Water Resour.*, 25, 1305–1312. [https://doi.org/10.1016/S0309-1708\(02\)00057-X](https://doi.org/10.1016/S0309-1708(02)00057-X)
- Santanello, J. A., Dirmeyer, P. A., Ferguson, C. R., Findell, K. L., Tawfik, A. B., Berg, A., et al. (2017). Land-atmosphere interactions: The LoCo perspective. *Bulletin of the American Meteorological Society*, 99(6), 1253–1272. <https://doi.org/10.1175/BAMS-D-17-0001.1>
- Seneviratne, S. I., Corti, T., Davin, E. L., Hirschi, M., Jaeger, E. B., Lehner, I., et al. (2010). Investigating soil moisture-climate interactions in a changing climate: A review. *Earth-Science Reviews*, 99(3–4), 125–161. <https://doi.org/10.1016/j.earscirev.2010.02.004>
- Taylor, C. M., Birch, C. E., Parker, D. J., Dixon, N., Guichard, F., Nikulin, G., & Lister, G. M. S. (2013). Modeling soil moisture-precipitation feedback in the Sahel: Importance of spatial scale versus convective parameterization. *Geophysical Research Letters*, 40, 6213–6218. <https://doi.org/10.1002/2013GL058511>
- Taylor, C. M., de Jeu, R. A. M., Guichard, F., Harris, P. P., & Dorigo, W. A. (2012). Afternoon rain more likely over drier soils. *Nature*, 489(7416), 423–426. <https://doi.org/10.1038/nature11377>
- Taylor, C. M., & Lebel, T. (1998). Observational evidence of persistent convective-scale rainfall patterns. *Monthly Weather Review*, 126(6), 1597–1607. [https://doi.org/10.1175/1520-0493\(1998\)126<1597:OEOPCS>2.0.CO;2](https://doi.org/10.1175/1520-0493(1998)126<1597:OEOPCS>2.0.CO;2)
- Taylor, C. M., Parker, D. J., Kalthoff, N., Gaertner, M. A., Philippon, N., Bastin, S., et al. (2011). New perspectives on land-atmosphere feedbacks from the African monsoon multidisciplinary analysis. *Atmospheric Science Letters*, 12(1), 38–44. <https://doi.org/10.1002/asl.336>
- Taylor, K. E., Stouffer, R. J., & Meehl, G. A. (2012). An overview of CMIP5 and the experiment design. *Bulletin of the American Meteorological Society*, 93(4), 485–498. <https://doi.org/10.1175/BAMS-D-11-00094.1>
- Tuttle, S. E., & Salvucci, G. D. (2017). Confounding factors in determining causal soil moisture-precipitation feedback. *Water Resources Research*, 53, 5531–5544. <https://doi.org/10.1002/2016WR019869>
- van der Ent, R. J., Savenije, H. H. G., Schaeffli, B., & Steele-Dunne, S. C. (2010). Origin and fate of atmospheric moisture over continents: Origin and fate of atmospheric moisture. *Water Resources Research*, 46, W09525. <https://doi.org/10.1029/2010WR009127>
- Voltaire, A., Sanchez-Gomez, E., Méliá, D. S. y., Decharme, B., Cassou, C., Sénési, S., et al. (2013). The CNRM-CM5.1 global climate model: Description and basic evaluation. *Climate Dynamics*, 40(9–10), 2091–2121. <https://doi.org/10.1007/s00382-011-1259-y>
- Volodin, E. M., Dianskii, N. A., & Gusev, A. V. (2010). Simulating present-day climate with the INMCM4.0 coupled model of the atmospheric and oceanic general circulations. *Izvestiya, Atmospheric and Oceanic Physics*, 46(4), 414–431. <https://doi.org/10.1134/S000143381004002X>
- Watanabe, M., Suzuki, T., O'ishi, R., Komuro, Y., Watanabe, S., Emori, S., et al. (2010). Improved climate simulation by MIROC5: Mean states, variability, and climate sensitivity. *Journal of Climate*, 23(23), 6312–6335. <https://doi.org/10.1175/2010JCLI3679.1>
- Yukimoto, S., Yoshimura, H., Hosaka, M., Sakami, T., Tsujino, H., Hirabara, M., et al. (2011). Meteorological Research Institute-Earth System Model Version 1 (MRI-ESM1)—Model description - (Tech. Rep. 64): METEOROLOGICAL RESEARCH INSTITUTE, JAPAN, Technical reports of the meteorological research institute.